N85-20454

SYNOPSIS OF MID-LATITUDE RADIO WAVE ABSORPTION IN EUROPE

K. M. Torkar

Space Research Institute of the Austrian Academy of Sciences
c/o Technical University of Graz
Inffeldgasse 12, A-8010 Graz
Austria

M. Friedrich

Department of Communications and Wave Propagation
Technical University of Graz
Inffeldgasse 12, A-8010 Graz
Austria

ABSTRACT

Radio wave absorption data covering almost two years from Europe to Central Asia are presented. They are normalised by relating them to a reference absorption. Every day these normalised data are fitted to a mathematical function of geographical location in order to obtain a daily synopsis of radio wave absorption. A film of these absorption charts was made which is intended to reveal movements of absorption or absorption anomaly. In addition, radiance (temperature) data from the lower D-region are also plotted onto these charts. No conclusions are drawn; the new procedure to evaluate absorption data is -- at the present stage of processing -- merely intended to stimulate discussion and interest.

INTRODUCTION

Radio wave absorption in the HF range occurs predominantly in the ionosphere's D-region, i.e. at heights where absorption L is proportional to both electron density and collision frequency ν. Since ν is very well predictable via atmospheric pressure (cf. e.g. FRIEDRICH and TORKAR, 1983) it is the electron density N_e which determines the day-to-day variations of L. At high latitudes all changes of N_e are attributable to variations of the ionising fluxes i.e. of charged particles; at low or middle latitudes, however, the fluxes responsible for the formation of the daytime D-region (solar Lyman-α, X-rays, etc.) do not vary drastically, not even in the course of a sunspot cycle. The observed day-to-day variations in (mid-latitude) radio wave absorption by factors of 2 to 3, notably in winter (winter anomaly), are therefore generally attributed to changes in the concentration of nitric oxide (NO), the only component of the middle atmosphere (mesosphere) which can be ionised by the relatively strong solar H Lyman-α line. The following analysis is plausible if one assumes that changes in the NO-concentration are the principal cause for changes of absorption.

DATA BASE AND NORMALISATION

There have been numerous attempts to study the morphology of winter anomalous absorption (e.g. BEYNON and WILLIAMS, 1976), in recent times notably by SATO (1981) who used f_{min} data from stations in Europe, the USSR and North America. The aim was to find a connection to geomagnetic activity, but the analysis is severely hampered by the relatively coarse classification of f_{min}.

In the present treatment we use absorption, i.e. loss of signal strength relative to absorption-free reflection. Both the methods A1 (vertical incidence) and A3 (oblique incidence, i.e. reception of a distant transmitter) are used. Table 1 gives the acronyms of the various data sets, path lengths,
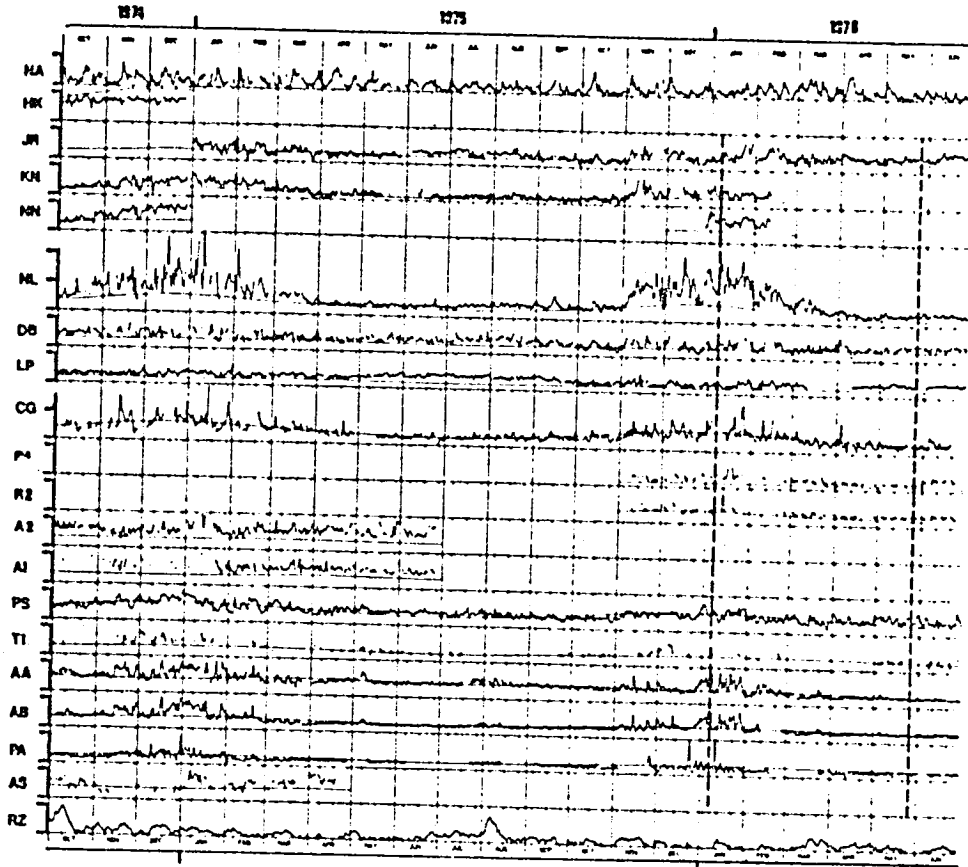
Figure 1. Absorption measurements of the available stations. NA is
the daily integrated riometer-absorption at Narssarssuaq, Greenland,
and RZ the Zurich sunspot number, all other acronyms are explained
in Table 1. Between bars indicates 60 dB, the smooth lines are
the simulated reference absorptions and the dashed lines show the
days used as examples for absorption patterns (Figure 3).

AA and AB which use the same transmitter but different receivers (distance of
the path mid-points ca. 120 km). Hence the observed rapid variations must be
considered to be of ionospheric origin and not -- as one might be tempted to
believe -- poorly maintained equipment or local interference.

Due to different path lengths, frequencies and the type of measurement
(daily integrated absorption L_D, noon-absorption L_{noon} etc.) the various data
sets show necessarily different seasonal trends and variabilities. Hence the
observed absorptions at various locations may be covered up by the above
mentioned, expected systematic effects. Therefore a procedure was sought by
which in a first approximation these differences can be eliminated.
Consequently a reference absorption for each data set and each month was cal-
culated. For this purpose electron densities were computed for the

Table 1.

		frequency MHz	distance km	type	weight summer	weight winter	geographic coordinates of midpoint	mean absorption height summer	mean absorption height winter
HK[1]	Hörby-Kühlungsborn	1.178	225	$\cos\chi = 0.2$	-	-	55.0N, 12.7E	92.72	90.13
JR	Juliusruh	2.000	-	noon	1.61	0.65	54.6N, 13.4E	91.24	104.08
KN	Kiel-Neustrelitz	2.775	220	$\cos\chi = 0.2$	0.42	0.75	53.9N, 11.6E	98.50	99.43
NN	Norddeich-Neustrelitz	2.614	395	$\cos\chi = 0.2$	-	1.05	53.5N, 10.1E	91.25	89.83
NL	Norddeich-Lindau	2.614	296	L_D [4]	0.93	0.77	52.8N, 8.7E	90.26	98.57
DB	De Bilt	1.850	-	noon	1.53	0.90	52.1N, 5.2E	90.89	96.47
LP[2]	Luxembourg-Prague	6.090	610	noon	-	-	50.1N, 10.3E	89.02	96.35
CG	Coburg-Graz	2.630	502	L_D	1.10	0.96	48.7N, 13.2E	87.69	95.29
R2	Rostov-on-Don	2.000	-	L_D	0.87	1.07	47.2N, 39.7E	92.73	93.96
R4	Rostov-on-Don	4.000	-	L_D	0.48	0.74	47.2N, 39.7E	83.35	83.13
A1	Alma Ata	1.700	-	noon	0.97	1.09	43.3N, 78.9E	88.57	89.55
A2	Alma Ata	2.200	-	noon	1.52	1.36	43.3N, 78.9E	90.73	93.04
PS	Priština-Sofia	1.412	170	$\cos\chi = 0.2$	0.71	1.26	42.7N, 22.2E	93.37	92.29
T1	Tbilisi	1.700	-	L_D	1.02	1.10	41.4N, 44.5E	90.38	92.97
AA	Aranjuez-El Arenosillo	2.830	424	noon[5]	0.90	1.07	38.6N, 5.2W	87.14	89.51
AB	Aranjuez-Balerma	2.630	374	L_D	1.13	1.17	38.4N, 3.2W	88.03	90.45
PA	Patras	[3]	[3]	L_D	0.87	1.05	38.0N, 23.8E	86.34[6]	88.96[6]
AS	Ashkhabad	1.800	-	noon	1.04	1.12	37.9N, 58.0E	88.98	89.94
								90.00	93.31

[1] not used in the further analysis, possibly ground wave propagation

[2] not used in the further analysis

[3] monitors the 31 and 49 m broadcast band; appr. linearly related to Rome-Athens on 6.080 MHz)
(ILIAS and GUPTA, 1979)

[4] except March 22 to June 30, 1976; $\cos\chi = 0.2$

[5] except December 1975 to February 1976; L_D

[6] applies to Rome-Athens

frequencies and (path mid-point) coordinates. Subject to the availability of the raw data, daily integrated absorption (L_D, cf. ROSE and WIDDEL, 1977), was used, otherwise values at noon or some constant solar zenith angle were employed. Figure 1 shows the daily values of all stations from October 1974 to June 1976.

The lowest curve is the sunspot number, whereas the uppermost curve represents the average daily riometer absorption at Narssarssuaq (Greenland). The latter is included as a measure of particle influx into the auroral zone, since a connection of charged particle fluxes and mid-latitude absorption has often been sought (e.g. MAEHLUM, 1967; TORKAR et al., 1980). However, only the northernmost data (JR) of February and October 1975 possibly show some direct influence of particles. On the other hand, even the relatively large sunspot numbers in August 1975 do not show up as enhanced absorption in any of the data. In most data one can clearly observe the larger absorption in winter, however, all show a larger variability in winter. Of special interest are the data sets

corresponding conditions of each station (noon, $\cos\chi = 0.2$ or at four typical solar zenith angles χ with equal time-spacing for L_p) using the ion-chemical model for low solar activity described elsewhere in detail (TORKAR and FRIEDRICH 1983). In this steady-state computation the neutral atmosphere, including the minor species, is taken from other published models, in particular [NO] from RUSCH et al. (1981). Absorption was then computed by a WKB ray-tracing calculation over a spherical Earth. The full SEN and WYLLER (1960) magnetoionic formulae were employed, the magnetic field taken from CAIN et al. (1967) and the collision frequency set proportional to pressure from the AFGL seasonal atmospheric model (COLE and KANTOR, 1978). The proportionality factor of 6.7×10^5 m^2 s^{-1} N^{-1} is the one recommended by FRIEDRICH and TORKAR (1983) based on a number of rocket measurements of ν. The reference absorption thus obtained is indicated in Figure 1 as smooth lines. Outside winter one can see reasonably good agreement for the data KN, NL, CG, TI, AA and AB. There is notably an excess of the simulated absorption of HK. This may be due to ground wave propagation at the fairly low frequency (1.178 MHz) of the path which is mainly over sea water. Another feature of the simulated absorption is, that at higher latitudes in summer the observed absorption ([NO]) is consistently higher than in the model (JR, KN, NL, DB, LP and also PS).

For further evaluation the daily absorption values were divided by the corresponding reference absorption. This new quantity (absorption enhancement AE) removes the different sensitivity of the various measurements provided the geometry of the ray (penetration into the ionosphere) is the same.

AE should, therefore, be proportional to an electron density ratio or the square of the ratio of ion production rates; if one assumes that NO and Lyman-α is the dominant production process of the absorbing D-region, AE is equal to $([NO]/[NO]_{ref})^2$.

Before combining all absorption measurements, normalized via AE in the above manner, it was tested to what extent the various data sets measure the same physical phenomenon. Figure 2 shows relative contributions of the various layers of height h to the total absorption of some of the stations using the reference ionosphere (summer), where $l_r(h)$ is defined as:

$$1_r = \frac{1(h)}{\int 1(h)\,dh} = \frac{1(h)}{L}; \quad \frac{dB/km}{dB}; \quad km^{-1}$$

One can see that the height regions contributing to absorption differ greatly from station to station. For want of more uniform data, all absorption measurements were nevertheless treated as if they represented the same height regions. Hence an absorption "drift" from e.g. JR to AS could just as well mean a downward motion of enhanced electron (or NO) density at both stations.

CONSTRUCTION OF ABSORPTION PATTERNS

The normalized data (absorption enhancement AE) still include variations due to very local effects. Instead of constructing AE-patterns by interpolation between the individual measurements, all AE-values were fitted by analytical functions. The number of locations, or -- more importantly -- the number of simultaneously available measurements, restricts the order of the analytical expression which can be fitted to the data. The simplest form is a plane in general position requiring only three, preferably evenly spaced, points. A somewhat higher level of complexity -- a circular paraboloid -- was chosen which is determined by four parameters, namely location and value of the maximum, and the curvature. This form is employed at the present stage of the analysis; higher orders have been tested, but found to lead to unrealistic excursions. In
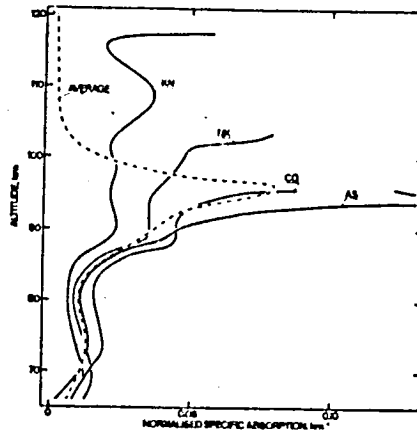
Figure 2. Relative absorption contributions of
different heights of some stations together with
the average absorption profile of all data sets
(summer).

an attempt to account for the different height coverages (cf. Figure 2) weights
w were given to the different data sets according to:

$$w = 1_r \int \overline{I} \, dh / \overline{I}^2 dh$$

Here $\overline{I}$ is the average specific absorption of all measurements divided by the
average integral absorption. Its height variation is also shown in Figure 2.
Table 1 contains these weights for January and July, but for the further
computation these weights were also established for all other months.

Furthermore contained in this table is the mean height of the absorption
derived from the same model computations. Those data which are based on
L_D $[= L_0/(1 + n)]$ were given additional daily weights according to the quality
of the fit $L = L_0 (\cos \chi)^n$ which led to the establishment of L_0 and n. For every
day four parameters were determined by fitting a paraboloid to all $\log(AE)$-
data by a least-mean-square procedure. In the film contours of absorption
enhancement of 0.8, 1.0, 1.3, 1.6 etc. are shown. In order to avoid too rapid
fluctuations of the absorption (AE-)patterns, running means of the four para-
meters are used, i.e. 50% of the day in question and 25% each of the previous
and following days.

The curves are fitted to the data in geographic Cartesian coordinates and
the contours of constant absorption enhancement then transformed to the
projection in which the satellite temperature data are available. In the film
only those stations which provided data on the day in question are indicated by
small circles. Figure 3 shows two examples where however, all possible stations
are indicated with their acronyms. From October 1975 on radiance (temperature)
data of the PMR (= Pressure Modulator Radiometer) of the University of Oxford
aboard the satellite NIMBUS-6 are available. The weighting function of the
highest channel 3000 peaks somewhere just below 80 km. The temperatures at that
height are surely not decisive for enhanced electron densities (electron loss
rates), but may be an indication of an unstable atmosphere, turbulence and — in
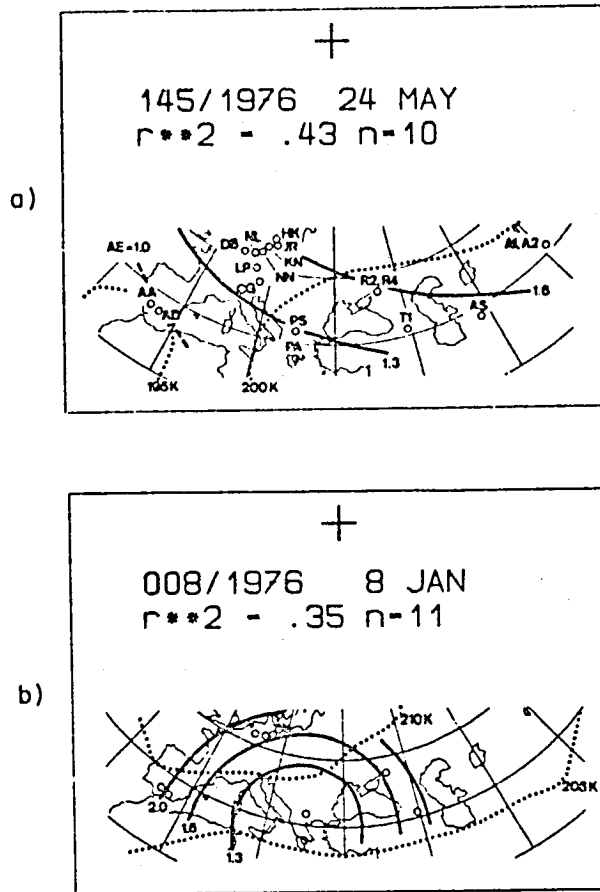consequence — of transport of NO into the D-region.

Figure 3. Examples of absorption patterns obtained
by fitting an analytical function to the AE values
and mesospheric temperatures. (a) typical summer,
May 24, 1976, (b) winter anomalous day January 8,
1976. r**2 is the quality of the fit and n the
number of available data for the day.

CONCLUSIONS AND IMPROVEMENTS

The quality of the presently available raw data does not permit to draw
final conclusions concerning the magnitude or the motions of absorption. More
careful screening of the absorption data is envisaged, but also the reference
absorption model, which mainly hinges on the adapted [NO]-model, may have to be
revised. For the derivation of velocities of absorption patterns it may perhaps
suffice to use the running mean as a reference, thereby avoiding errors intro-
duced by an unrepresentative reference absorption.

ACKNOWLEDGEMENTS

REFERENCES

Beynon, W. J. G. and E. R. Williams (1976), J. Atmos. Terr. Phys., 38, 89.
Cain, S. H., S. J. Hendricks, R. A. Langel and W. V. Hudson (1967), J. Geomagn. Geoelect., 19, 335.
Cole, A. E. and A. J. Kantor (1978), Air Force Reference Atmosphere, AF-GL-TR-78-0051.
Friedrich, M. and K. M. Torkar (1983), J. Atmos. Terr. Phys., 45, 267.
Ilias, D. J. and G. P. Gupta (1979), J. Atmos. Terr. Phys., 41, 601.
Maehlum, B. N. (1967), J. Geophys. Res., 72, 2287.
Rose, G. and H. U. Widdel (1977), J. Atmos. Terr. Phys., 39, 51.
Rusch, D. W., R. G. Roble, J.-C. Gerard and A. I. Stewart (1981), in Handbook for MAP, Vol. 2 (ed. by S. K. Avery), pp. 442-449.
Sato, T. (1981), J. Geophys. Res., 86, 9137.
Sen, H. K. and A. A. Wyller (1960), J. Geophys. Res., 65, 3931.
Torkar, K. M. and M. Friedrich (1983), J. Atmos. Terr. Phys., 45, 369.